Controlled Molecularly Mediated Assembly of Gold Nanooctahedra for a Glucose Biosensor

Xing-Jiu Huang,*,† Cun-Cheng Li,‡ Bonsang Gu,† Ju-hyun Kim,† Sung-Oh Cho,‡ and Yang-Kyu Choi*,†

Nano-Oriented Bio-Electronic Lab, School of Electrical Engineering and Computer Science, and Department of Nuclear and Quantum Engineering, Korea Advanced Institute of Science and Technology, Daejeon, 305-701, South Korea

Received: October 17, 2007; In Final Form: December 17, 2007

This article describes the controllable construction of a layered superstructure of gold nanooctahedra via a molecularly mediated assembly and their electrochemical application as a host matrix toward the oxidation of glucose. The layered superstructures of the Au nanooctahedra were confirmed with atomic force microscopy, X-ray electron spectroscopy, and cyclic voltammograms. The effects of the interface of gold spherical nanoparticles and the different layered interface of gold nanooctahedra on the electrochemical responses to $Fe(CN)_6^{3-}$ and glucose were investigated in detail. The glucose biosensor, which uses the Au nanooctahedra layer structure as a matrix, shows excellent electrocatalytic activities, such as a high level of sensitivity, a fast response, and a wide response range.

Downloaded via UNIV OF JINAN on September 21, 2018 at 12:24:13 (UTC).
See https://pubs.acs.org/sharingguidelines for options on how to legitimately share published articles.

1. Introduction

Immobilization of biomolecules in designer-made nanoscale structures can significantly improve the performance of biocatalytic processes.[1] From the point of view of efficient biocatalytic processes, the candidates of nanostructure materials with a high loading, high active surface area, and long-term stability, as well as high electron transfer are very useful.[1,2] Owing to their large surface area, gold spherical nanoparticles modified on a conductive substrate have gained much attention with regard to the construction of an electrochemical sensing interface.[3−6] In addition, the presence of sharp edges or tips in faceted metal nanoparticles has been demonstrated to be useful for enhancing electric fields, which is important for applications such as sensors.[7] Raj, Shi, and co-workers have suggested that the high electrocatalytic activity of gold particles can be ascribed not only to surface area; surface morphology and shape also play an important role, such as flowerlike morphology.[8] Recently, a new class of extremely regular Au nanocrystals with sharp edges or corners, the nanooctahedron, has been successfully synthesized.[9] Unfortunately, previous studies on the potential application of the nanooctahedron have usually focused on surface-enhanced Raman scattering and optical properties.[9d,e] Our goal in this article, which is an extension of our previous report on the high-yield synthesis of single-crystalline gold nanooctahedra,[9a] is to controllably construct a layered superstructure of gold nanooctahedra via a molecularly mediated assembly and to investigate the application of the assembly as a host matrix for a glucose sensor.

2. Experimental Procedures

Materials. We obtained poly(vinylpyrrolidone) (PVP, K-30, M_w = 40 000), poly(ethylene glycol) 600 (PEG 600, M_w = 570−600), $AuCl_3$, and 1,8-octanedithiol (≥97%) from Aldrich. In addition, we purchased glucose oxidase (GOx, EC 1.1.3.4), D-(+)-glucose, and agarose from Sigma. Next, we prepared a phosphate-buffered saline solution (PBS, pH 7.4) by dissolving 1.6 g of KCl, 64 g of NaCl, 1.92 g of KH_2PO_4, and 11.52 g of K_2HPO_4 in 800 mL of double deionized water (DDW). All chemicals were used as received. We also purchased gold (2 mm in diameter), Ag/AgCl (saturated KCl solution), and a Pt wire electrode from CH Instruments, Inc.

Synthesis of Gold Nanooctahedra. Octahedral gold nanocrystals were synthesized in a PEG 600 solution via a modified polyol process.[9a] For a typical synthesis, 0.05 mL of 100 mM of sodium borohydride ($NaBH_4$) was introduced to a 20-mL PEG 600 solution of PVP (222 mg) before the addition of gold (III) chloride ($AuCl_3$, 0.16 mL, 125 mM) aqueous solution. The final concentrations were about 1 mM for the gold (III) ions, 0.25 mM for the $NaBH_4$, and 100 mM for the PVP. The gold precursor solution was transferred into an oil bath and first preheated at 75 °C for more than 24 h, followed by further heating at 125 °C for 6 h. In the initial preheating step, the $NaBH_4$ acts as a strong reducing agent that directly reduces the gold (III) ions in the solution to gold (0) atoms. However, only part of the gold (III) ions was reduced to gold (0) atoms because the concentration of $NaBH_4$ was under a stoichiometric condition (that is, where the mole ratio of Au/$NaBH_4$ is 1:0.25). The as-formed gold (0) atoms or clusters were then oxidized by the remaining gold (III) ions via the following reaction:

$$\text{gold (III)} + 2\text{gold (0)} \rightarrow 3\text{gold (I)}$$

Hence, most of the gold (III) ions finally evolve to gold (I) ions via the preheating process. As a result, the absorption band in the UV spectrum for gold (III) ions completely disappears and the plasmon band for the Au nanocrystals does not appear. Consequently, the preheating gold precursor is colorless. In the second heating process, the gold (I) ions are reduced to gold (0) atoms via the polyol process for a reaction temperature greater than 100 °C; this process subsequently produces the gold nanocrystals. In this case, the PEG 600 serves not only as a solvent of the precursors but also as a reducing agent for the

* Corresponding authors. Telephone: 82-42-869-8077. E-mail: xingjiuhuang@hotmail.com; ykchoi@ee.kaist.ac.kr.
† School of Electrical Engineering and Computer Science.
‡ Department of Nuclear and Quantum Engineering.

10.1021/jp710112q CCC: $40.75 © 2008 American Chemical Society
Published on Web 02/15/2008

reaction. Finally, we collected the products by centrifugation (15000 rpm) and then washed them repeatedly with ethanol for examination and application.

Molecularly Mediated Assembly of Gold Nanooctahedra. The Au electrodes were used as working electrodes. Before the assembly, the gold electrodes were polished with 0.05-μm alumina, sonicated for 2 min, and then rinsed thoroughly with DDW and dried in a stream of high-purity N_2. The activated Au electrode was first functionalized with 1,8-octanedithiol (0.1 M) to produce a thiol group-terminated surface, which was treated with an ethanol solution of 1,8-octanedithiol. The gold nanooctahedron assembled electrode was obtained by placing a freshly 1,8-octanedithiol-modified gold electrode into a gold nanooctahedra ethanol solution for 6 h under ambient conditions. The thiol forms a covalent link to a gold nanooctahedron surface. The modified electrode was then washed sequentially with ethanol and DDW under ultrasonication to eliminate any possible physical absorbed impurities and other gold nanooctahedra. The gold nanooctahedra were therefore assembled on the substrate by means of the Au−S chemical bond. This process was repeated five times until a set of Au nanooctahedra-modified electrodes were obtained with different layers. It is important to note here that the condensation reactions between the double thiol groups are not considered due to the shorter carbon chains. For comparison purposes, we also used the same process to prepare an electrode modified with a monolayer of gold spherical particles (approximately 40 nm in diameter).

Enzyme Electrode Preparation. To guarantee the compatibility of the electrode, we prepared the enzyme electrode using the gold nanooctahedra layered structure after $Fe(CN)_6^{3-}$ experiments. The enzyme was immobilized onto the DDW-washed electrode surface by deposition of 2.5-μL droplets of a glucose oxidase solution (2.5 mg mL^{-1}). The enzyme electrode was then allowed to dry in air for 4 h. After the glucose oxidase was immobilized on the electrode, we stabilized it by using a 2.5-μL aliquot of agarose hydrogel (0.2 mg mL^{-1}). Finally, we thoroughly washed the Au octahedra/GOx/agarose with a cold buffer and stored it at 4 °C.

Electrochemical Measurements. The cyclic voltammetry measurements were performed with a CHI 600B electrochemical analyzer (CH Instruments, Inc.). In addition, the amperometry was performed with a BAS 50W voltammetric analyzer (Bioanalytical System, Inc.). All the electrochemical experiments were carried out in a PBS solution in a conventional three-electrode cell at room temperature. We also used Ag/AgCl as a reference and Pt wire as a counter electrode.

Characterization. Atomic force microscopy (AFM) was done with a Nanoscope (Digital Instruments, Veeco Metrology) scanning probe microscope. Field emission scanning electron microscopy (FESEM) images were obtained with a Philips XL 30 AFEG scanning electron microscope, and transmission electron microscopy (TEM) images were obtained with an FEI Tecnai F20. X-ray electron spectroscopy (XPS) was carried out by electron spectroscopy for chemical analysis 2000.

3. Results and Discussion

Observations with TEM were used to demonstrate that the Au nanoparticles were formed in a parallelogram shape (Figure 1A). The corresponding image of FESEM (as shown in the lower right of inset of Figure 1A) clearly shows that a majority of the as-prepared product is made up of octahedral Au nanoparticles. Furthermore, in each octahedron all eight faces are equilateral triangles and four triangles meet at each corner. The average length of the edge of the octahedral nanoparticles

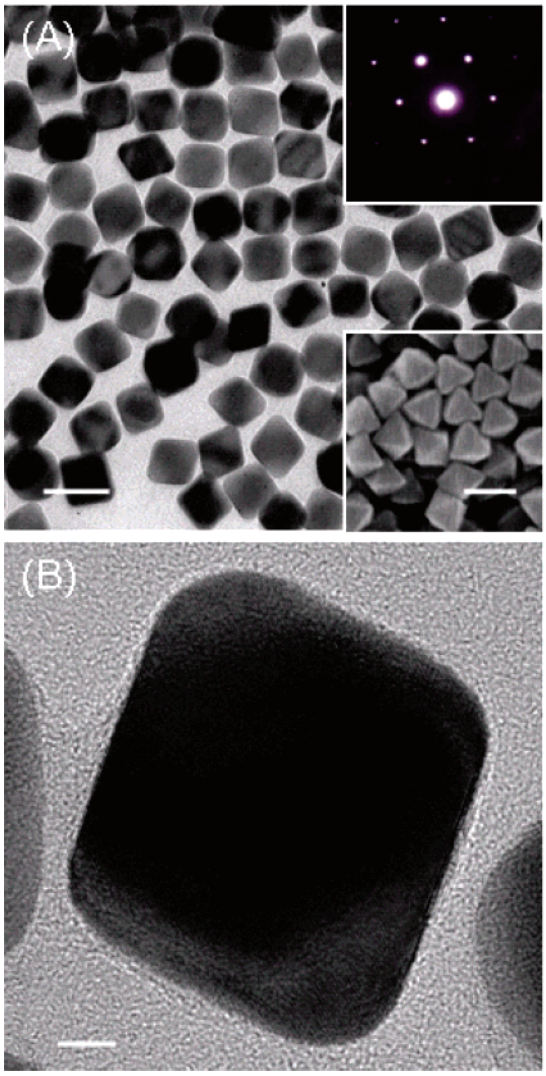

Figure 1. Typical TEM (A) and HRTEM (B) images of gold nanooctahedra. The scale bars for (A) and (B) are 50 and 5 nm, respectively. The inset in (A) (lower right) clearly shows the FESEM image of the gold nanooctahedra corresponding to (A), in which the scale bar is 50 nm. The inset in (A) (upper right) shows the electron diffraction pattern of an individual octahedral particle.

was approximately 40 nm, and the polydispersity was less than 10%. The selected area electron diffraction (the upper right of the inset of Figure 1A) and high-resolution TEM (HRTEM, Figure 1B) for a single particle both indicate that the as-prepared gold nanoparticles are composed of single crystals.

As illustrated in Figure 2A, the layered superstructures of Au nanooctahedra were constructed onto an Au electrode surface via a 1,8-octanedithiol-mediated assembly. By using stepwise treatments of the superstructure with the Au nanooctahedra solution and the molecular mediator, we were able to generate interfaces of a controllable number of layers. Considering that the strength among the layers is from Au−S covalent bond, the resulting molecular-mediated Au nanooctahedra superstructures are very stable and the particles can only be removed from the surface by physical scratching. The glucose oxidase is then immobilized on the surface of Au nanooctahedra superstructures. As a result, the Au nanooctahedra layers electrically contact the active site of the adjacent enzyme layer and the electrode. Figure 2B shows the corresponding atomic model of the controlled molecularly mediated assembly.

The layered superstructures of the Au nanooctahedra were confirmed with AFM, XPS, and cyclic voltammograms. The

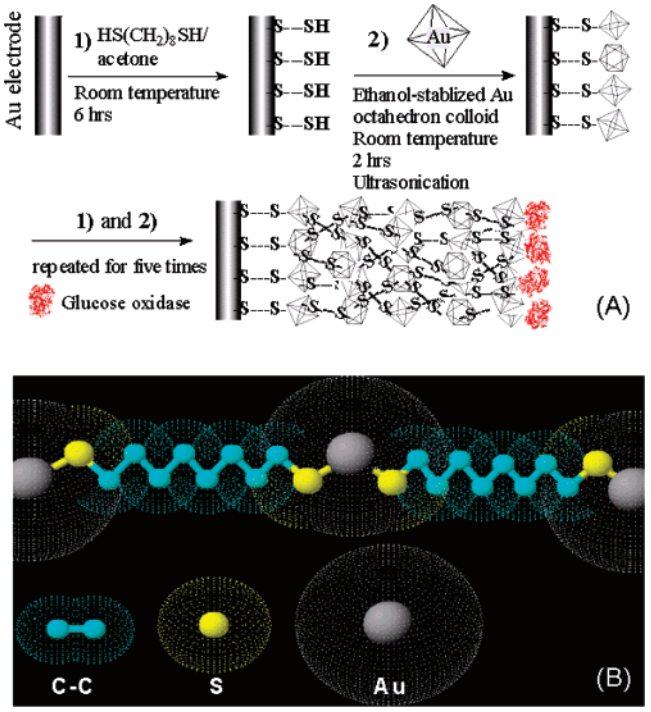

Figure 2. (A) Schematic illustration of the stepwise controlled molecularly mediated assembly of gold nanooctahedra and glucose oxidase. (B) Atomic model of the controlled molecularly mediated assembly.

surface properties of the molecular-mediated assembly of the Au nanooctahedra layers were first characterized with AFM height images and the corresponding cross-sectional analysis. Because of the difficulty in obtaining AFM images of the commercial gold electrode surface, we performed AFM measurements on exposed patterned gold surfaces. The Au pattern was prepared on a 4-in. p-type silicon wafer with a photolithography technique. Figure 3A,B shows the typical AFM height image of the superstructures on a stepwise assembly of a single layer (A) and five layers (B). From the interface of the patterned gold and silicon, we can clearly distinguish the different manner between this molecular-mediated assembly and the physical adsorption method (the nature of which is considered to be electrostatic). After being ultrasonicated, few Au nanooctahedra can be observed on the surface of the silicon wafer; the particles only assemble on a gold surface. In addition, the increases in height as shown by AFM can be attributed to the growth of the number of layers. This situation is clearly supported when we analyze cross sections of the samples (Figure 3C). The cross sections reveal that the multilayered Au nanooctahedra form an interdigitated fine structure rather than a simple platelike structure on the surface of the substrate. This result suggests that the assembly via a molecular mediator proceeds along a direction different from that of Au nanooctahedra. For the second layer, we cannot observe an obvious sawtooth structure. This outcome occurs probably because the first layer cannot cover the electrode surface with a higher density during the assembling time and the second layer consequently fills the gaps among the particles. Compared with the physical adsorption method, the molecular-mediated assembly has the advantage of overcoming the stack tendency in a face-to-face manner during the physical adsorption process.[10] In addition, we conducted an XPS experiment on this molecular-mediated assembly of Au nanooctahedra to confirm key information concerning the chemical state of the film surface. Figure 4 shows the wide-scan spectra and high-resolution $S2p_{1/2}$ and O1s

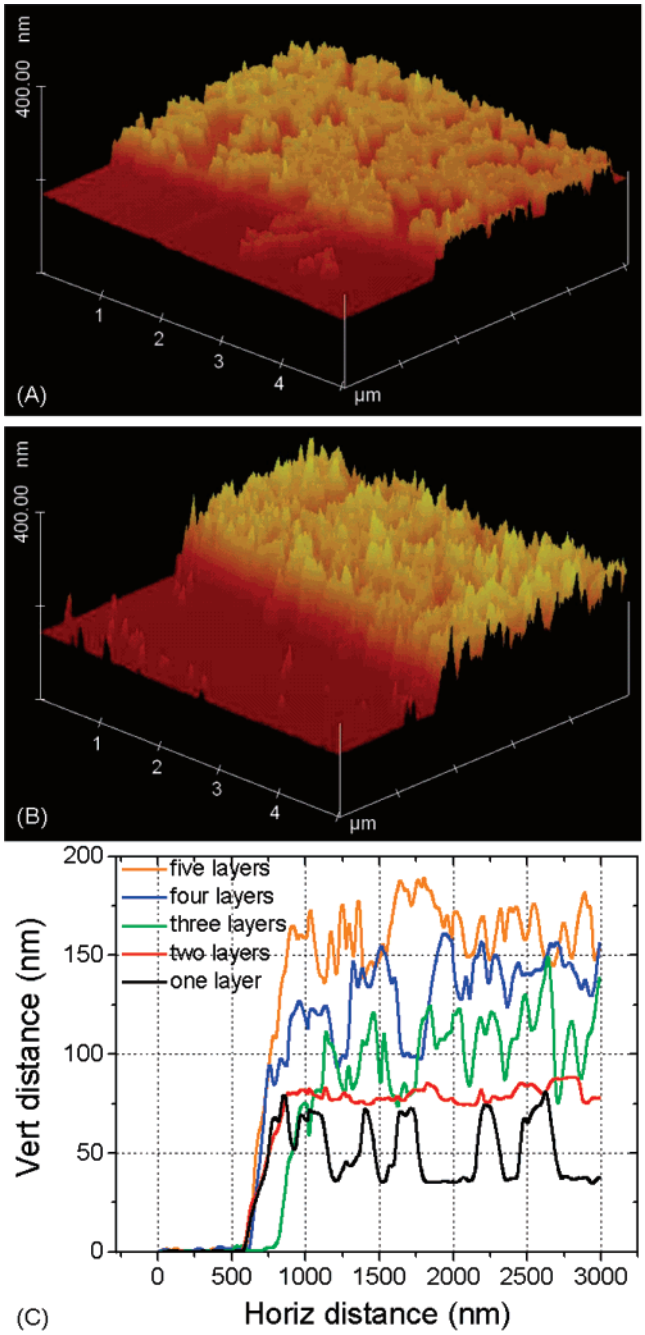

Figure 3. Typical tapping mode AFM height image of single-layer (A) and five-layer (B) molecularly mediated assembly of gold nanooctahedra. (C) Typical cross section of different gold layers in AFM images.

spectra. From the survey scans, we can observe the $S2p_{1/2}$ signal, which demonstrates that HS groups have been successfully introduced onto the surface of the Au particles. The appearance of a very weak peak of O1s can be attributed to ethanol on the surface of the nanooctahedra; ethanol is used to prevent the Au nanooctahedra from agglomerating.

To check whether the molecular-mediated layered superstructure of Au nanooctahedra can be used as a host matrix for enzyme immobilization, we investigated the electrochemical behavior of ferricyanide, which is widely used as an electrochemical probe at the surface of layered superstructures. Figure 5A presents cyclic voltammograms of the Au nanooctahedra surfaces in assemblies containing one to five layers. As stated in the outlet, gold spherical nanoparticles can also be used to construct an electrochemical sensing interface through modifica-

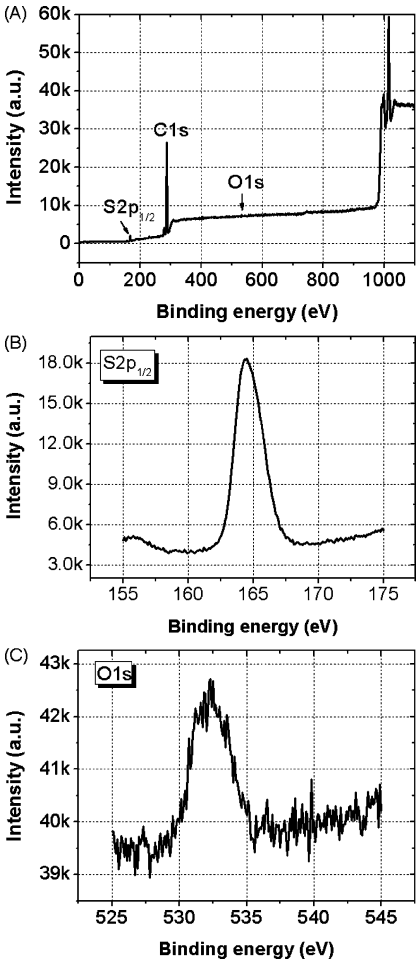

Figure 4. (A) XPS wide-scan spectrum of gold substrate after molecularly mediated assembly of gold nanooctahedra. (B, C) High-resolution $S2p_{1/2}$ and O1s spectra, respectively.

tion of a conductive substrate. We therefore prepared one layer of gold spherical particles and nanooctahedra in a manner identical to that described in the Experimental Procedures. The cyclic voltammograms are found in curves c (blue, spherical particles) and d (black, octahedra) of Figure 5A. We found an increase in the response current for one layer of the nanooctahedra electrode. For this shape-dependent response, it is worthwhile to compare the surface density and roughness of the nanooctahedral layer and the spherical particles. As observed in Figure 3C, the low surface density is considered because the first layer of nanooctahedra could not cover the entire electrode surface, whereas spherical particles easily form a nearly packed monolayer. However, the surface in the nanooctahedral has a greater mean roughness, $R_a = 13.689$ nm, compared with that of spherical particles, $R_a = 9.143$ nm. This voltammetric feature should, therefore, be explained by considering the unique shape of the octahedral; that is, the sharp edges or corners are useful for an electrochemical reaction. In another comparison with the bare Au electrode, we found that the response current of both the Au spherical particles and the Au nanooctahedra electrode was deservedly higher because of the increased surface area. Furthermore, the fact that a voltmmetric response could not be observed for the $HS(CH_2)_8S-Au$ electrode reveals that the electron transfer between the metal substrate and the analyte in a solution is almost totally hindered by the monolayer, possibly due to the length of thiol chain self-assembled monolayer.[11] After assembling the gold nanoparticles, we found that the electrochemical behavior may be due to a fine-tuning effect of

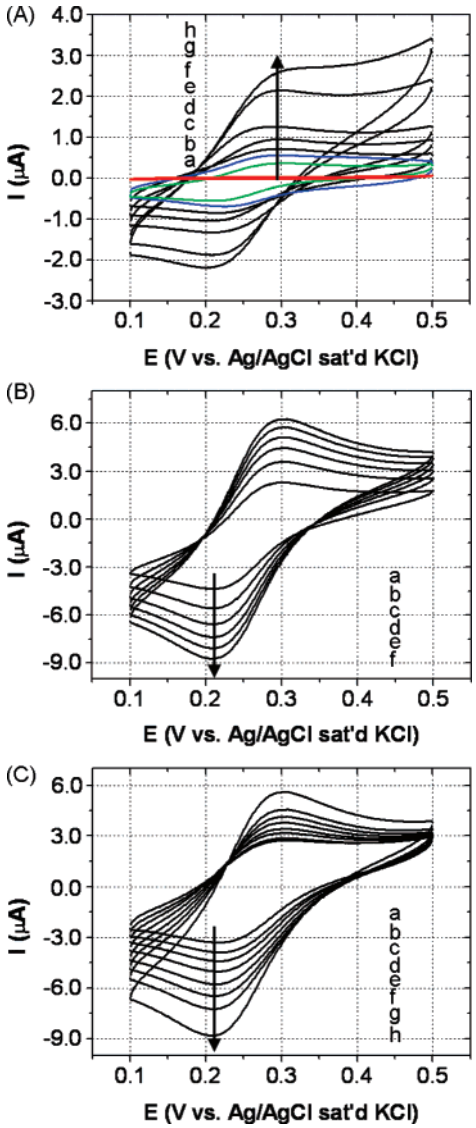

Figure 5. (A) Cyclic voltammograms of the layered Au particle assemblies in 0.1 mM $Fe(CN)_6^{3-}$/PBS (pH 7.4). Sweep rate: 40 mV s^{-1}. (a) Flat Au surface with a SAM layer (red); (b) bare flat Au electrode (green); (c) single-layered Au spherical particles (blue); (d−h) one to five layers of Au nanooctahedra (black). (B) Cyclic voltammograms of five-layered Au nanooctahedra under different sweep rates in 0.8 mM $Fe(CN)_6^{3-}$/PBS (pH 7.4). (a) 5, (b) 10, (c) 15, (d) 20, (e) 25, and (f) 30 mV s^{-1}. (C) Cyclic voltammograms of five-layered Au nanooctahedra under different $Fe(CN)_6^{3-}$ concentrations. (a) 0.1, (b) 0.2, (c) 0.3, (d) 0.4, (e) 0.5, (f) 0.6, (g) 0.7, and (h) 0.8 mM. Sweep rate: 40 mV s^{-1}.

gold nanoparticles at the electrode.[12] Last, we observed that the response current increases with the growth of the number of layers (as shown by curves d−h in Figure 5A). This phenomenon, which can be explained by the fact that the surface area or coverage increases as the growth of the number of layers increases, is confirmed by the increased capacitance. This point is in excellent agreement with previously reported results that state that the surface area of an assembly of Au spherical particles increases almost linearly as the number of layers increases,[3] and that catalytic reactions are more favorable with a high nanoparticle coverage.[8a,13]

A five-layered Au nanooctahedra assembly was selected to sense ferricyanide at different sweep rates. Figure 5B shows the cyclic voltammograms. The anodic current and the cathodic current are linearly proportional to the sweep rates ($I_{pa} = 1.912 + 0.156\upsilon$; $I_{pc} = -3.741 - 0.173\upsilon$, where υ is the sweep rate

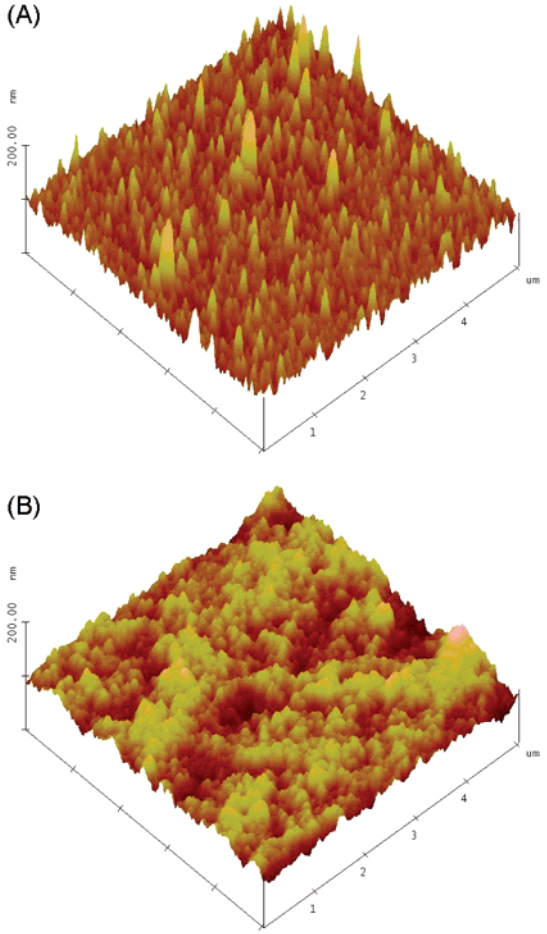

Figure 6. Typical tapping mode AFM height image of GOx immobilized on a Au nanooctahedra surface. (A) Single-layered Au nanooctahedra with 2.5 μL of 2.5 mg/mL glucose oxidase. (B) GOx is stabilized by agarose hydrogel.

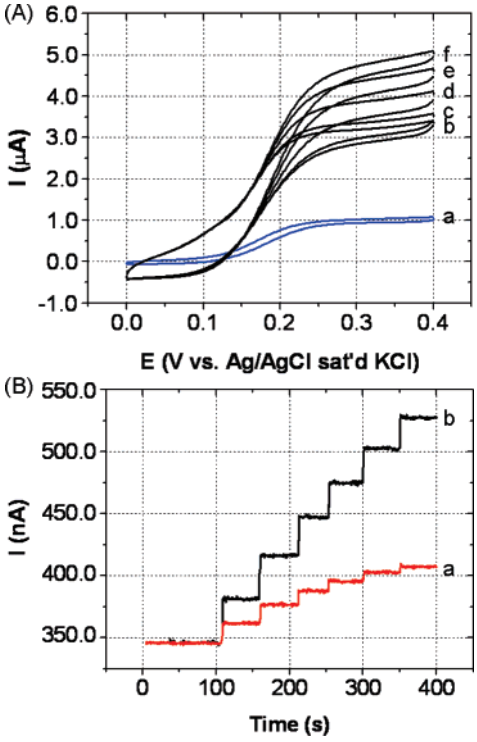

Figure 7. (A) Cyclic voltammograms of single-layered Au particle/GOx assemblies in glucose/PBS at a sweep rate of 20 mV s^{-1}. (a) Single-layered Au spherical particle/GOx system in 7.8 mM of glucose. (b−f) Single-layered Au nanooctahedra/GOx system in different concentrations of glucose: (b) 7.8, (c) 8.6, (d) 9.4, (e) 11.2, and (f) 12 mM. (B) Current responses of a single-layered (a) and a five-layered (b) Au nanooctahedra/GOx system upon successive additions of 0.01 M glucose aliquots (50 μL each). The initial potential was 250 mV, the sensitivity was 1×10^{-9} A V^{-1}, and the measurement was performed in 4 mL of PBS (pH 7.4) while being stirred.

(V s^{-1})), indicating that the electrode kinetics is controlled by a surface-adsorption electrochemical process. Figure 5C shows cyclic voltammograms of a five-layered Au nanooctahedra assembly at different concentrations. As the bulk concentration of ferrocyanide increases, the voltammetric response is stably enhanced, demonstrating that there is no dissociation of nanooctahedra from the electrode surface. From these cyclic voltammogram measurements, therefore, we conclude that the layered superstructures of the molecular-mediated assembly of nanooctahedra exhibit high stability and do not easily peel off from the electrode surface when placed in a solution.

Similarly, owing to the difficulty in taking AFM images of the immobilized GOx with biochemical activity on the layered structure surface, we performed AFM measurements on exposed layered Au nanooctahedra surfaces prepared in a manner identical to the procedure described in Figure 2A. Figure 6A displays the result after the immobilization of GOx on a single-layered surface of Au nanooctahedra. Considering that the height of the enzyme unit is about 5 nm,[14] we confirmed that several enzyme units agglomerate and form a multilayer on the octahedral surface. In other words, the surface area of single-layered Au nanooctahedra is not enough for immobilization of 2.5 μL of 2.5 mg mL^{-1} glucose oxidase. As a result, the nanooctahedra only electrically contact the active site of the adjacent enzyme layer and the electrode. In addition to having moderate mechanical strength and high stability in an aqueous solution, agarose hydrogel film has relatively good stability in some solvents, such as dimethylsulfoxide, ethanol, and dioxane.[15] Thus, agarose hydrogel film is useful for constructing an effective enzyme film, particularly organic phase biosensors.[15] Next, we stabilized the GOx units that were assembled on the surface of electrode by using 2.5 μL of 0.2 g L^{-1} agarose hydrogel. Figure 6B shows the surface morphology in an AFM image. By observing the height of images A and B, we can easily deduce that the agarose hydrogel wraps the enzyme surface tightly and forms a thin layer of several nanometers. We also found that pure agarose hydrogel film has a porous network structure with a diameter of 50−100 nm (data not shown). These features improve the contact between the sample and the surface of the enzyme better and guarantee the electron transportation from the enzymatic active center to the electrode through the Au nanooctahedra.

Figure 7A highlights the comparative results of the cyclic voltammograms for the single-layered Au nanooctahedra/GOx system and spherical particles/GOx system. The dependence on the shape of the Au particles can be clearly observed (curves a to b), that is, the single-layered Au nanooctahedra/GOx system (curve b) exhibits a greater voltammetric response current at the potential of 0.25 mV than the single-layered spherical particles/GOx system under the same conditions. Although the mechanism of the shape-controlled electrical contacting of the enzyme redox center and the electrode is, at present, not fully understood, this result clearly indicates that, as a matrix for enzyme loading, Au nanooctahedra seems better than spherical particles. It should be pointed out, however, that highly efficient electrical contacting of the enzyme needs a reconstitution of the enzyme on nanoparticles.[16] Here, it is also important to consider that the excellent electrical contacting of the enzyme

redox center and the nanooctahedra may be due to the mediator of $Fe(CN)_6^{3-}$, which is from previous experiments before enzyme immobilization. With the aid of $Fe(CN)_6^{3-}$, the electrons are transported through the Au nanooctahedra from the enzymatic active center to the electrode. Furthermore, the results show a substantial increase in the electrochemical capacitance of the single-layered Au nanooctahedra/GOx system. The capacitance was calculated from the cyclic voltammogram curves, with $C = i/\upsilon$, where i is the current and υ is the sweep rate ($V\ s^{-1}$). At a potential of 0.1 V, for example, the effective capacitance is about six times larger than that of the single-layered Au nanooctahedra/GOx system. This high capacitance, which is consistent with the large surface area,[17] demonstrates that the Au nanooctahedra/GOx system can provide a larger surface area for the electrochemical reaction. The surface coverage and roughness of single-layer nanooctahedral and spherical particles have been discussed before. We deduce, therefore, that such an octahedral structure with large surface geometrically and crucially affects the electrochemical behavior of the surface.

To continue to probe the effect of Au nanooctahedra layer on voltammetric response, we investigated the real-time current−concentration behavior of glucose for the single-layered and five-layered Au nanooctahedra/GOx system at a constant electrode potential of 250 mV where the oxidation current peak of glucose appears shown in Figure 7A. The results are presented in Figure 7B. In these two cases, the current increases stepwise with each successive addition of the glucose solution. The response is very fast in reaching a dynamic equilibrium upon each addition of the sample solution, generating a steady-state current signal within several seconds. This fast response can be explained by the fact that the nanosizes and the unique octahedral structure lead to the effective electron transfer from the substrate to products through the octahedral matrixes that contain enzymes. The steady-state current signal in each stairway indicates that another extremely attractive feature of this system is the highly stable amperometric response toward glucose.

The typical plots of the response current versus concentration are linear for the single-layered and five-layered Au nanooctahedra/GOx system (Figure 8A). However, the calibration plot for the single-layered Au nanooctahedra/GOx system has a slope of 0.07 $\mu A\ mM^{-1}$ (sensitivity) and a correlation coefficient of 0.981, whereas the five-layered Au nanooctahedra/GOx system has a slope of 0.233 $\mu A\ mM^{-1}$ and a correlation coefficient of 0.998. Note also that the sensitivity of each electrode varies slightly because of differences in the enzyme loading for each electrode. We suggest therefore that under the same enzyme loading the response depends on the layer of Au octahedra, and that higher responses are obtained with higher layers. A higher layered structure provides a higher surface area, which can accommodate much more glucose oxidase in a given region. Consequently, we can expect a higher level of sensitivity. This suggestion, as shown in Figure 8B, is further supported by the response range of the single-layered Au nanooctahedra/GOx system. Figure 8B shows a linear plot of the response current of the single-layered Au nanooctahedra/GOx system versus the glucose concentration. The plot has a slope of 0.349 $\mu A\ mM^{-1}$ and a correlation coefficient of 0.998 over a wide concentration range of 0.125 to 12 mM. No saturation current is observed due to the larger surface coverage of the GOx units. The sensitivity over the wide response range is increased because of the lower concentration. Actually, the sensitivity of 0.07 $\mu A\ mM^{-1}$ in the range of 0.125 to 0.75 mM implies that the Au octahedral/GOx system exhibits a higher affinity for glucose sensing.

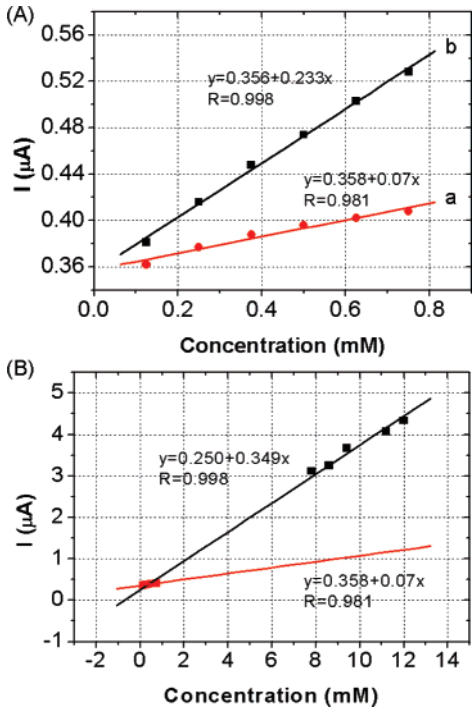

Figure 8. (A) Plots of chronoamperometric current versus the glucose concentration for a single-layered (a) and a five-layered (b) Au nanooctahedra/GOx system and corresponding linear calibration curves. (B) Plots of the chronoamperometric current versus a wide concentration range of glucose for a single-layered Au nanooctahedra/GOx system and the corresponding linear calibration curve.

4. Conclusions

Our construction of a layered superstructure via a molecular-mediated assembly demonstrates the application of Au nanooctahedra in electrochemistry. We have successfully demonstrated the possibility of the structure being used as a host matrix for enzyme immobilization. With the help of $Fe(CN)_6^{3-}$, the nanooctahedra act as good nanoconnectors that electrically contact the active center of the enzyme and the electrode, resulting in high electron transfer and high biocatalytic efficiency. The glucose biosensor, which uses the Au nanooctahedra layer structure as a matrix, shows a high level of sensitivity (0.349 $\mu A\ mM^{-1}$ over a wide concentration range of 0.125 to 12 mM), a fast response (within several seconds), and a wide response range (from 0.125 to 12 mM). On the basis of these results and the inherent features of the structure, we can expect such a layered superstructure of Au nanooctahedra formed via molecular-mediated assembly to be a useful matrix for the immobilization of any other enzymes. Moreover, it can be used for various biocatalytic and bioelectrocatalytic detection.

Acknowledgment. X.-J.H. expresses appreciation for the financial support of the Brain Korea 21 project, the School of Information Technology, and the Korea Advanced Institute of Science and Technology in 2007. Also, this work was partially supported by the NRL program of the Korea Science and Engineering Foundation grant funded by the Korean government (MOST) (No. R0A-2007-000-20028-0).

References and Notes

(1) Lee, D.; Lee, J.; Kim, J.; Kim, J.; Na, H. B.; Kim, B.; Shin, C. H.; Kwak, J. H.; Dohnalkova, A.; Grate, J. W.; Hyeon, T.; Kim, H. S. *Adv. Mater.* **2005**, *17*, 2828−2833.

(2) Teng, X.; Liang, X.; Rahman, S.; Yang, H. *Adv. Mater.* **2005**, *17*, 2237−2241.

(3) (a) Lahav, M.; Shipway, A. N.; Willner, I.; Nielsen, M. B.; Stoddart, J. F. *J. Electroanal. Chem.* **2000**, *482*, 217−221. (b) Lahav, M.; Gabai, R.; Shipway, A. N.; Willner, I. *Chem. Commun.* **1999**, 1937−1938. (c) Shipway, A. N.; Lahav, M.; Blonder, R.; Willner, I. *Chem. Mater.* **1999**, *11*, 13−15. (d) Lahav, M.; Gabriel, T.; Shipway, A. N.; Willner, I. *J. Am. Chem. Soc.* **1999**, *121*, 258−259. (e) Lahav, M.; Shipway, A. N.; Willner, I. *J. Chem. Soc., Perkin Trans.* **1999**, *2*, 1925−1931. (f) Doron, A.; Katz, E.; Willner, I. *Langmuir* **1995**, *11*, 1313−1317.

(4) (a) Gittins, D. I.; Bethell, D.; Nichols, R. J.; Schiffrin, D. J. *Adv. Mater.* **1999**, *11*, 737−740. (b) Bethell, D.; Brust, M.; Schiffiin, D. J.; Kiely, C. *J. Electroanal. Chem.* **1996**, *409*, 137−143.

(5) (a) Abdelrahman, A. I.; Mohammad, A. M.; Okajima, T.; Ohsaka, T. *J. Phys. Chem. B* **2006**, *110*, 2798−2803. (b) Raj, C. R.; Abdelrahman, A. I.; Ohsaka, T. *Electrochem. Commun.* **2005**, *7*, 888−893.

(6) (a) Zhang, H.; Lu, H. Y.; Hu, N. F. *J. Phys. Chem. B* **2006**, *110*, 2171−2179. (b) Dai, X.; Nekrassova, O.; Hyde, M. E.; Compton, R. G. *Anal. Chem.* **2004**, *76*, 5924−5929. (c) Hu, X. Y.; Xiao, Y.; Chen, H. Y. *J. Electroanal. Chem.* **1999**, *466*, 26−30. (d) Finot, M. O.; Braybrook, G. D.; McDermott, M. T. *J. Electroanal. Chem.* **1999**, *466*, 234−241.

(7) (a) Sánchez-Iglesias, A.; Pastoriza-Santos, I.; Pérez-Juste, J.; Rorígueez-González, B.; Abajo, F. J. G.; Liz-Marzán, L. M. *Adv. Mater.* **2006**, *18*, 2529−2534. (b) Kelly, K. L.; Coronado, E.; Zhao, L. L.; Schatz, G. C. *J. Phys. Chem. B* **2003**, *107*, 668−677.

(8) (a) Jena, B. K.; Raj, C. R. *Langmuir* **2007**, *23*, 4064−4070. (b) Li, Y.; Shi, G. Q. *J. Phys. Chem. B* **2005**, *109*, 23787−23793.

(9) (a) Li, C. C.; Shuford, K. L.; Park, Q. H.; Cai, W. P.; Li, Y.; Lee, E. J.; Cho, S. O. *Angew. Chem., Int. Ed.* **2007**, *46*, 3264−3268. (b) Zhang, J.; Liu, H.; Wang, Z.; Ming, N. *Appl. Phys. Lett.* **2007**, *90*, 163122−163124. (c) Seo, D.; Park, J. C.; Song, H. *J. Am. Chem. Soc.* **2006**, *128*, 14863−14870. (d) Sánchez-Iglesias, A.; Pastoriza-Santos, I.; Pérez-Juste, J.; Rorígueez-González, B.; Abajo, F. J. G.; Liz-Marzán, L. M. *Adv. Mater.* **2006**, *18*, 2529−2534. (e) Zhang, J. G.; Gao, Y.; Alvarez-Puebla, R. A.; Buriak, J. M.; Fenniri, H. *Adv. Mater.* **2006**, *18*, 3233−3237.

(10) Xue, C.; Li, Z.; Mirkin, C. A. *Small* **2005**, *1*, 513−516.

(11) Huang, X. J.; Im, H. S.; Yarimaga, O.; Kim, J. H.; Lee, D. H.; Kim, H. S.; Choi, Y. K. *J. Phys. Chem. B* **2006**, *110*, 21850−21856.

(12) Cheng, W. L.; Dong, S. J.; Wang, E. K. *Langmuir* **2002**, *18*, 9947−9952.

(13) Kumar, S.; Zou, S. Z. *J. Phys. Chem. B* **2005**, *109*, 15707−15713.

(14) Patolsky, F.; Weizmann, Y.; Willner, I. *Angew. Chem., Int. Ed.* **2004**, *43*, 2113−2117.

(15) Liu, H. H.; Tian, Z. Q.; Lu, Z. X.; Zhang, Z. L.; Zhang, M.; Pang, D. W. *Biosens. Bioelectron.* **2004**, *20*, 294−304.

(16) (a) Xiao, Y.; Patolsky, F.; Katz, E.; Hainfeld, J. F.; Willner, I. *Science* **2003**, *299*, 1877−1881. (b) Zayats, M.; Katz, E.; Baron, R.; Willner, I. *J. Am. Chem. Soc.* **2005**, *127*, 12400−12406.

(17) Liu, C. Y.; Bard, A. J.; Wudl, F.; Weitz, I.; Heath, J. R. *Electrochem. Solid-State Lett.* **1999**, *2*, 577−578.